Novel scanning near-field optical microscope (SNOM)/scanning confocal optical microscope based on normal force distance regulation and bent etched fiber tips

J. F. Wolf, P. E. Hillner,[a] R. Bilewicz, P. Kölsch, and J. P. Rabe
Humboldt University Berlin, Institute of Physics, Physics of Macromolecules, Invalidenstrasse 110, 10115 Berlin, Germany

(Received 29 December 1998; accepted for publication 5 March 1999)

We report on a unique combination of a novel scanning near-field optical microscope/scanning confocal optical microscope based on normal force distance regulation with bent etched fiber tips. The use of normal force detection makes all classic atomic force microscope operation modes such as contact mode and tapping mode accessible to scanning near-field optical microscopy (SNOM), thus allowing near-field optical imaging at sample distances unavailable to shear force regulated distance control. The SNOM laser light is pulsed or detected synchronously to the fiber tapping amplitude to illuminate the sample at a predetermined height above the sample. Bent etched fiber tips are used, whose fiber diameters are additionally etched down to yield resonant frequencies between 60 and 300 kHz, *Q* factors around 180 and spring constants in the range of 80–400 N/m. The typical roughness of the tip cone surfaces is shown to be due to etching in a meniscus. For the first time, simultaneously acquired constant gap width mode topography and constant height mode near-field optical images are presented, allowing topography induced contrast to be separated from true optical contrast such as absorption and fluorescence. © *1999 American Institute of Physics.* [S0034-6748(99)03506-6]

I. INTRODUCTION

Recently, a growing awareness has developed in the scanning near-field optical microscope (SNOM) community of the danger of topography induced artifacts influencing or even dominating the contrast in SNOM images.[1] This problem is exacerbated by the goal of imaging ever smaller structures with ever weaker optical contrast.[2] Also, smaller apertures and structures have evanescent fields which decay over smaller distances, making smaller tip sample distances even down to contact desirable.[2] On the other hand, Hecht *et al.* have shown that *z* motion of the tip down to even 1 Å generates visible contrast in the SNOM signal.[1] Basically, this means that a SNOM can be viewed as an atomic force microscope (AFM) with a ''functionalized tip'' and a good SNOM must be a good AFM in the first place. This concept was the driving force behind the design of our SNOM. We tried to optimize the design along the following criteria which characterize a high resolution AFM: high *z* sensitivity, high stability against vibrations, and low thermal drift. In order to be able to check the images for true optical contrast free of artifacts, we furthermore incorporated a confocal scanning optical microscope (''classical optics'') and the ability to use standard AFM tips (''classical topography'') into our SNOM design.

The vast majority of SNOMs utilizes shear force distance detection.[3–5] Besides being not as well understood as normal force distance detection, it has a minimum working distance of 5–10 nm.[5] A few other groups also use normal force detection for their SNOMs.[6–9] Lewis *et al.*[8] also have a combined scanning confocal optical microscope, but use pulled fiber tips, as do Talley *et al.*[9] The other groups[6,7,9] do not have the confocal optical microscope capability and use single tube scanners whose scan curvature at large scan ranges make them less suited to confocal optical microscopy than our design. The simultaneous acquisition of topography in constant gap width mode and near-field optical information in constant height mode is demonstrated here for the first time. Hecht *et al.*[1] showed images where the constant height mode (CHM) optical image was acquired after the constant gap width mode (CGM) topographical image. Our simultaneous acquisition is superior, because it eliminates thermal drift and tip change effects as much as possible and thus enables a separation of topographically induced contrast from true optical contrast such as absorption or fluorescence.

The combination of a SNOM with normal force distance detection, bent etched fiber tips, and integrated scanning confocal optical microscope is thus unique and with the novel data acquisition mode provides an instrument with high *z* sensitivity, high intensity near-field illumination, and links to well-understood classical contrast mechanisms, well suited for the study of weak contrast structures.

The article is structured as follows: In part II some general considerations will be presented which were the basis of our instrument design. In part III we describe the design of our scanner, then in part IV we discuss the tip production. Finally, we show simultaneously acquired CGM topography and CHM near-field optical images and summarize the results.

[a]Present address: Box 0450, University of California at San Francisco, San Francisco, CA 94143-0450.

II. GENERAL CONSIDERATIONS

After realizing that a SNOM is basically an AFM with ''functionalized tips,'' our goal was to build a highly stable AFM as the basis for our SNOM. The vast majority of SNOMs use a feedback based on shear force detection.[3–5,10] The understanding of this detection method is, however, not complete. The tip sample distance in feedback is around 5–10 nm. In contrast, the distance detection method of choice for classical AFMs is based on sensing normal force and it is used on virtually all AFMs. Hence the understanding of the feedback mechanism and the interpretation of the resulting images is well advanced and progressing rapidly due to the large AFM community. The adoption of new techniques such as the tapping mode or imaging under liquids[11] has opened up the use of AFMs in the fields of soft and in particular biological samples. Resolution in the z direction is around 0.1 nm and the tip sample distance in feedback can be from contact to true noncontact in the tens of nm range. This allows near-field optical imaging at small sample distances unavailable to shear force regulated distance control, and these distances will become more and more important as SNOM resolution improves.[2] Previous experience with a shear force detection SNOM revealed difficulties tracking the surface at large scan ranges of a few tens of microns, which were not a problem for normal force AFMs. Therefore, we chose to use a normal force detection-based AFM as the basis for our SNOM. The main feedback mode should be tapping mode, as the SNOM will be primarily used for thin organic films. At the same time, that meant modifying the standard fiber tips used in SNOM to make them useable in a normal force AFM as will be described later. Changing the geometry of the fiber tips to that of a cantilever also greatly enhances the lifetime of a fiber tip in the microscope, since the tip can react to sample contacts by deflecting away and thus not be destroyed. In addition, our microscope can be used with commercially available bent pulled fiber tips (Nanonics), as well as with future cantilever-based SNOM tips as they become commercially available.[12,13]

III. SCANNER DESIGN

Our SNOM scanner is situated on an inverted microscope (Zeiss Axiovert 135TV), which collects the light emitted from the tip for transmission mode SNOM (see Fig. 1). It features a symmetric design for good intrinsic thermal drift compensation, similar to earlier scanning tunneling microscope (STM) designs which are known for their high thermal and mechanical stability.[14–16] A number of later designs for low/variable temperature, high resolution work[17–20] have been based on the original ''stand alone'' beetle design.[16] This is the first time this highly stable scanner design has been used for SNOM. High stability is of great importance for SNOM as well, especially when low light levels and weak contrast dictate long integration periods for the optical signal.

Our SNOM scanner consists of three piezo tubes arranged on a circle which support and scan the sample (see Fig. 2). With our controller (Digital Instruments Nanoscope IIIa), scan ranges of 29 μm^2 and a z range of 3.9 μm are possible. In the center of the circle is an invar tube which supports the stationary cantilever, which can be either a bent SNOM tip or a standard AFM cantilever. The displacement of the cantilever is detected using optical beam deflection. The focusing optics are mounted in the center tube. They focus the laser diode beam down to an 8 μm spot on the backside of the cantilever that can be positioned within a

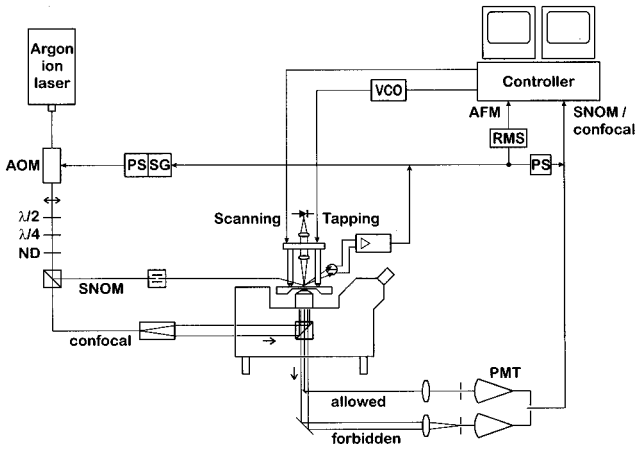

FIG. 1. Schematic view of the instrument setup. The SNOM is situated on an inverse microscope, which collects the light in transmission. The light from the scanning confocal microscope is collected in reflection. The laser light can be modulated relative to the tapping frequency of the cantilever, or the PMT signal can be measured phase sensitive to the tapping cantilever. The abbreviations are: AOM, acoustic optical modulator; ND, neutral density filter; PS, phase shifter; SG, signal generator; VCO, voltage controlled oscillator; RMS, root mean square generator; PMT, photo multiplier tube.

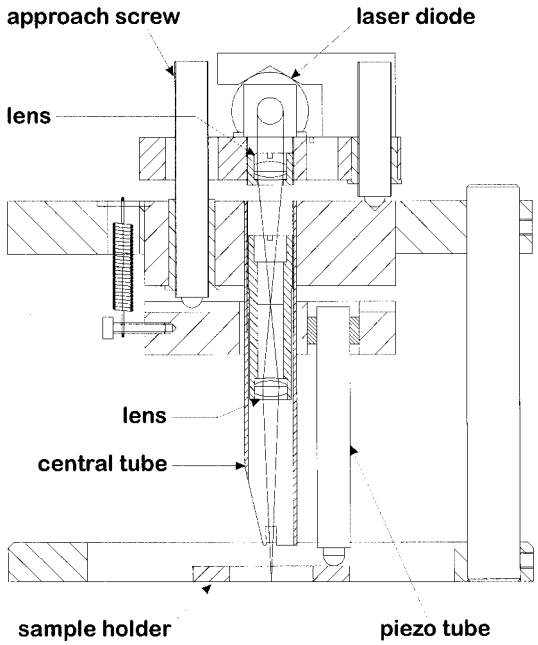

FIG. 2. Cross-sectional view of the SNOM scanner. The sample is attached to the bottom side of the sample holder. The piezo tubes (only the one in the cross-sectional plane shown for sake of clarity) are arranged symmetrically on a circle and support the sample holder with magnetic half spheres attached to the ends of the tubes. The cantilever (not shown here for sake of clarity) is mounted on the end of a central tube positioned in the center of the three piezo tubes. The laser beam from the feedback laser diode is focused onto the backside of the cantilever with two lenses. The reflected beam is detected on a position-sensitive photodiode (not shown).

circle of 8 mm diameter. In addition, the quadrant photodetector can be placed anywhere in a solid angle of 80° by 50°. These two features are very important and useful when using homemade tips, whose geometry is more subject to variations than commercial AFM tips. Apart from the controller, the electronics are homebuilt, including a tapping signal generator compatible with the Nanoscope tapping mode software protocol.

In previous work of Cleveland *et al.*,[21] laser diode light emitted from a glass fiber was used to illuminate the cantilever instead of the usual free optical beam. This resulted in a greatly reduced $1/f$ noise and made possible the first time measurement of hydration potentials with AFM. Our setup is designed to be able to switch back and forth between both free beam and fiber illumination modes. Laser diodes of different wavelength can also be exchanged easily.

The sample holder is attached magnetically to three half spheres glued onto the bottom of the piezo tubes. It can be manually approached towards the tip over a range of many millimeters with three fine screws. These can also be used to eliminate sample tilt and thus align the scan plane horizontally to the focal plane of the inverted microscope. Using three piezo tubes greatly reduces the scan curvature normally present with a single large scan range tube scanner. This is of great importance with respect to the combined scanning confocal optical microscope, as it ensures the sample surface is in focus over the whole scan range and thus prevents artifacts. The sample can be laterally fine positioned under the tip using the inertial slider algorithm in the Nanoscope software.

A free laser beam can be directed into the reverse side of the inverted microscope and focused into a spot on the sample from below. Since the sample is scanned, this can be used for a scanning confocal laser microscope in reflection mode. Having the tip stationary is also advantageous for the optical alignment and prevents artifacts due to the tip scanning out of the focus of the collection lens.[1] The collected light is detected by a photomultiplier tube (Hammamatsu R928).

The use of an oil immersion lens on the inverted microscope not only improves the collection efficiency of the transmitted or fluorescent light, it also can be used to collect the so called forbidden light, which is normally not accessible to nonimmersion lenses in combination with microscope slide shaped sample substrates. The oil immersion lens translates the various propagation cone angles of the transmitted light into various radii in the collimated beam behind the lens, as has also been mentioned by Hecht *et al.*[22] The allowed and forbidden light can then be separated by a mirror of appropriate dimension placed in the beam path.

When operated in tapping mode, the SNOM tip is at a constantly varying distance from the sample. This means that, due to the distance dependence of the light as well as the optical resolution, one is effectively averaging over the various intensities and resolutions connected with the sweep through the complete tapping amplitude. In order to eliminate this effect, one can pulse the light synchronously to the tapping cantilever.[6] This could, however, have the side effect of exciting unwanted vibrational amplitude in the cantilever because of thermal response of the tip.[23] Another possibility is to detect the photomultiplier current synchronously to the tapping cantilever. In both methods one can introduce phase lags and thus in effect measure SNOM images at various distances from the surface, ranging from contact to the maximum tapping amplitude. We have provided for both methods, but have not implemented them yet in the images shown in this article.

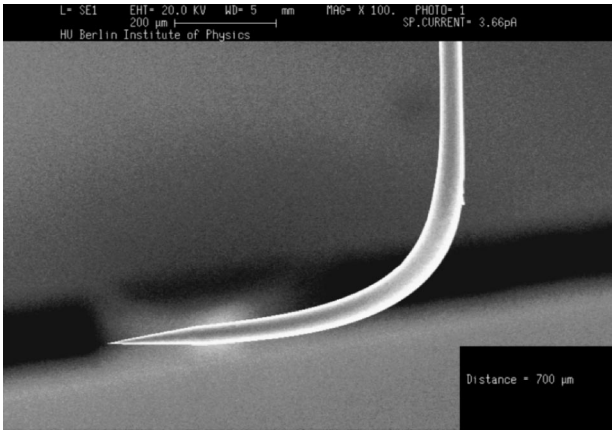

FIG. 3. SEM image of a bent fiber with a tip subsequently etched at the end. Scale bar at top of image is 200 μm. The distance of 700 μm denotes the length of the fiber from the tip to the bend.

IV. TIP PRODUCTION

The vast majority of tips used in SNOM are pulled glass fiber tips as developed by Betzig *et al.*[24] Recently, however, glass fiber tips produced by etching techniques have been shown to be capable of superior transmission ratios of up to two orders of magnitude higher than comparable pulled tips.[25] We therefore chose to use the etching technique for our tips as well.

Prior to etching, the fibers need to be bent in order to obtain the cantilever geometry. This is done by positioning the fiber in the beam of a CO_2 laser and heating with a laser pulse of given time and power. By varying these parameters, it is possible to achieve bend angles of $100° \pm 1°$, which is the angle necessary due to the design of our scanner. The radius of the bend is on the order of 500 μm. An example of such a cantilevered fiber tip is shown in Fig. 3.

For soft samples like organic films, care has to be taken to image with a cantilever having an appropriate force constant. Typical force constants and resonance frequencies for tapping mode levers are 20–100 N/m and 200–400 kHz, respectively. To achieve these force constants with a fiber lever, either the total length of the fiber extending over the lever mount must be over 3 mm, resulting in resonance frequencies below 20 kHz, or the fiber diameter has to be thinned down. With diameters of 35 μm and a cantilever length of 0.6 mm, the calculated force constant is 80 N/m and the resonance frequency is 80 kHz (for these calculations, a simple model of a straight cylindrical rod was used, ignoring the mass of the bent down portion of fiber). To thin down the fibers, they are simply immersed in pure HF for an amount of time prior to the etching of the tip. The Q factor was measured to be around 180.

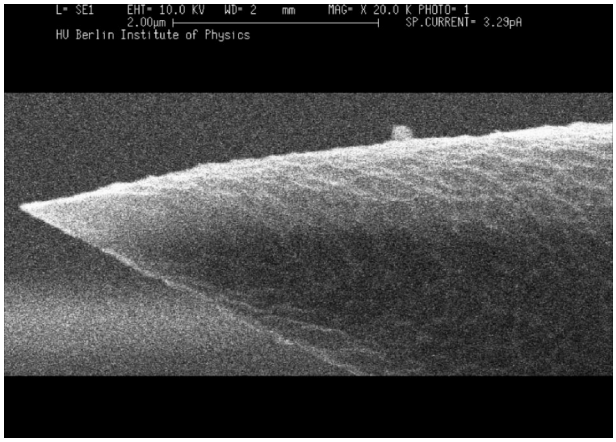

FIG. 4. SEM image of a tip etched in pure 40% HF with a protection layer of hexadecane. The tip radius is below 50 nm, while the surface roughness on the cone area is estimated to be below 30 nm. Scale bar at top of image is 2 μm.

After the fiber is bent, the tip is etched using the protection layer technique.[26] Using hexadecane as the protection layer and pure 40% HF as the etchant, we have achieved tip radii of under 50 nm (Fig. 4). The cone angle of the tip is $\sim$40° and the taper region $\sim$200 μm long.

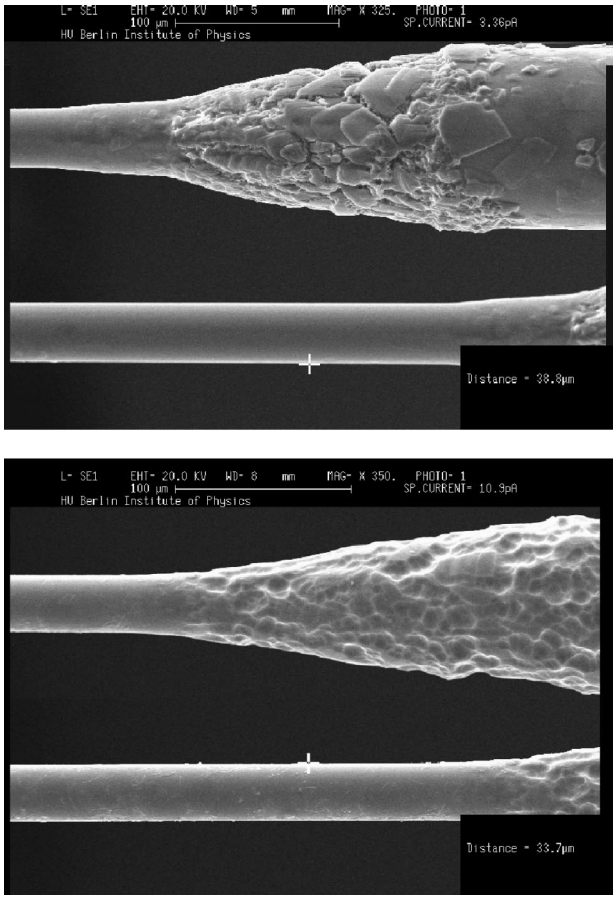

FIG. 5. Two different fibers etched in parallel in a buffered HF solution with a protection layer of hexadecane and withdrawn before complete tip formation. The etch time was 132 min. The much greater roughness on the cone surfaces in comparison to the flat cylindrical areas is evident. The scale bar in both images is 100 μm, the distance values denotes the diameter of the remaining fibers respectively.

The side walls of the tips show the typical roughness as has been seen by many groups, on the order of below 30 nm. Inspection of the surface roughness of the thinned down regions in the scanning electron microscope (SEM) showed only the roughness of the thin gold coating necessary for the SEM imaging. This is in stark contrast to the roughness present on the tip side walls. Obviously, the roughness is not due to the HF etching *per se*, but to the etching in the reduced volume of the meniscus. In a recent article, it was suggested the roughness came from the finite mixing of the HF etchant and the protection layer, and it was shown that reducing the total etching time could reduce the roughness.[27] In our opinion, this cannot be the only explanation, as it does not explain why we only see the roughness of the gold layer on the thinned down parts of our fiber tips.

We tested different etching solutions with very different etching rates, the first being a buffered HF solution known for creating very smooth surfaces, the second being pure 50% HF. The buffered HF solution consisted of two parts buffered HF (7:1), one part deionized water, one part acetic acid, and one part 40% HF and had an etching rate of 300–350 nm/min. The acetic acid and deionized water components help dissolve the accumulation of residuals on the fiber surface during the etching process.[28] Inspection in the SEM (Fig. 5) revealed a much rougher cone surface than with pure 40% HF. It looked as if the fiber consisted at least on the outer regions of single crystallites, the edges of which had been worked out by the etching process. In contrast, the 50% HF solution (Fig. 6) not only etched much faster (2.5 μm/min), but produced more cylindrically symmetric tips with a lower tip cone roughness than the 40% HF solution (1.2 μm/min). This suggests that (a) the glass fibers are not completely amorphous and (b) the pure 50% HF solution is a much more isotropic etchant than the buffered solution. If the fiber has any residual crystallinity, an as isotropic as possible etchant is what is needed. However, even with the 50% HF solution, the surface roughness on the tip cone surfaces is still higher than on the areas where the fiber was merely thinned down, without the presence of a meniscus. Therefore, we conclude that the meniscus itself must have an

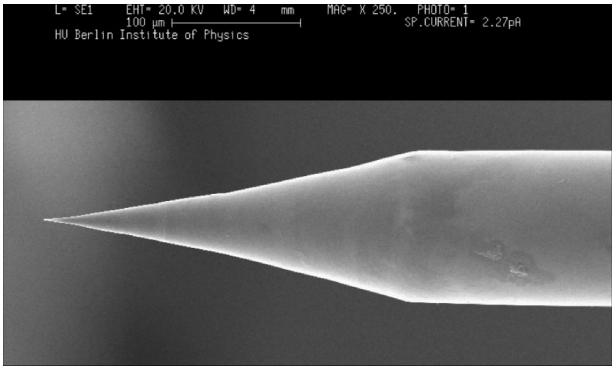

FIG. 6. SEM image of a tip etched in pure 50% HF with a protection layer of hexadecane. The etching solution was kept at a constant temperature of 30 °C, the etch time was 25 min. The cone surfaces are much smoother and more symmetrical than those prepared with the buffered etch solution. The scale bar is 100 μm.

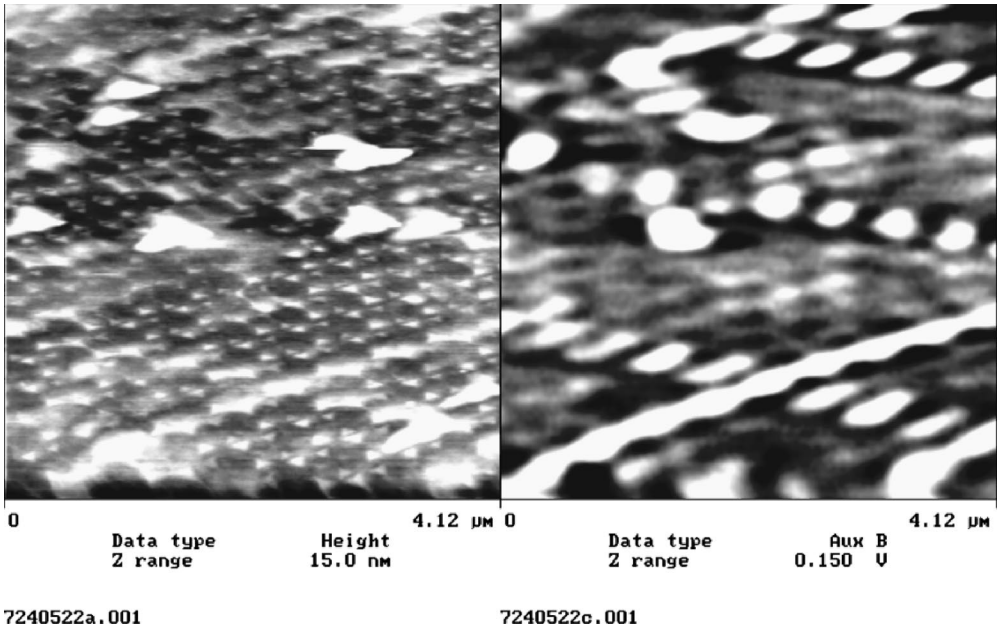

FIG. 7. Topography (height, left) and transmission near-field optical (Aux B, right) image of the latex sphere shadow mask sample. The grayscale of the optical image is inverted and is scaled in arbitrary units. Thus, areas of higher absorption appear brighter, making the comparison with the topographical image easier. The small triangular islands are well resolved, albeit with a double tip. The optical image was recorded in constant height mode, with the tip retracted from the surface by 12 nm. There are no double tip effects visible. The resolution is estimated to be on the order of 80 nm.

influence on the resulting surface roughness, possibly through the constricted volume and resulting buildup of concentration gradients.

One might expect that introducing a bend into the fiber would completely destroy the polarization state of light emitted from the tip. However, other groups[29] working with straight fiber tips found that the polarization is mainly destroyed by unsymmetrical apertures, an equal problem for both bent and straight fiber tips. In fact, a recent article[30] showed that a bend in the fiber does not completely destroy the polarization of the emitted light, but that comparable extinction ratios to straight fiber tips can be achieved even with bent fiber tips in cantilever geometry (70:1). Our tests so far have not been as successful, obtaining extinction ratios of 10:1. As stated, this could be mainly due to unsymmetrical apertures.

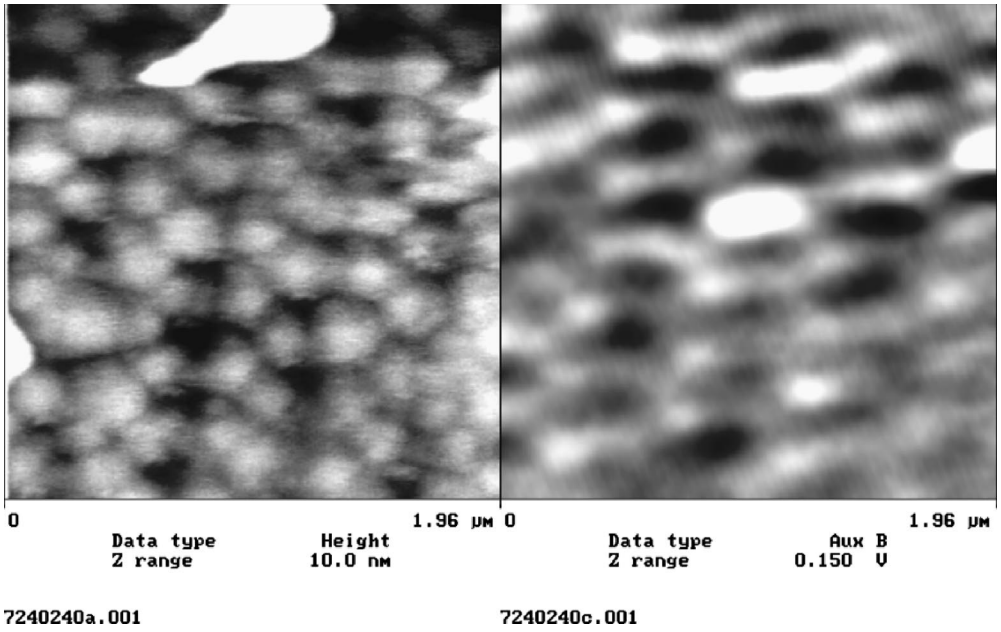

FIG. 8. Topography (height, left) and transmission near-field optical (Aux B, right) image of the latex sphere shadow mask sample. The grayscale of the optical image is inverted and is scaled in arbitrary units. Thus, areas of higher absorption appear brighter, making the comparison with the topographical image easier. The tip has changed since the image in Fig. 7, it is no longer a double tip, but the resolution has degraded and the triangular shape of the small islands is not clearly resolved any more. The resolution in the optical image is still estimated to be on the order of 80 nm. The large contamination bump at the top of the topographical image is not visible in the SNOM image.

V. FIRST RESULTS

As pointed out by Hecht *et al.*,[1] the easiest way to obtain SNOM images free of feedback induced artifacts is to collect the data in constant height mode, i.e., with the feedback loop turned off. That way, intensity variations due to tip distance changes caused by the feedback loop working at the higher topography resolution cannot occur. However, in this collection mode the intensity variations due to varying tip-surface distances are maximized, albeit with the lateral optical resolution of the SNOM tip. In effect, the intensity of the light illuminating the sample is no longer constant. In order to discern contributions from the true optical properties of the sample and those stemming from sample topography, one must know the topography as precisely as possible. Therefore, we collected the data in the following fashion: first, the topography data is collected with the feedback loop set to track the corrugation as exactly as possible. Then, the tip scans over the same line in a second pass to collect the SNOM data. In this second pass, the tip retracts by a given amount from the surface and then scans horizontally across the surface with the feedback loop completely turned off. This is different from the so called lift mode used, e.g., in magnetic force microscopy, where the tip in the retracted scan retraces the topographical contour. Afterwards, the tip proceeds to the next line and first scans the topography and then the SNOM image and so forth. In this way, we have both good topography information and SNOM data free from feedback induced artifacts.

The results shown in Figs. 7 and 8 are images of a latex sphere shadow mask[31] (sample courtesy of U. Ch. Fischer, Univ. Münster). To prepare the sample, a droplet of latex spheres in solution is put on a glass substrate. After evaporation of the solvent, a thin aluminum film is deposited to the glass substrate, covering not only the latex spheres, but also the spaces in between them. Subsequently, the latex spheres are removed in an ultrasonicator, leaving behind a pattern of aluminum islands. The radius of the latex spheres on our sample was 453 nm, the thickness of the aluminum layer was 10–20 nm. The size of the triangular islands is around 180 nm.

The topographic image was taken in tapping mode with a Nanonics tip having a resonance frequency of 398 kHz. The SNOM images were taken in transmission mode, the Nanonics tips having a nominal aperture of 50 nm. The tip was retracted by 12 nm from the surface for the SNOM scan line. The larger islands are clearly visible as dips in the intensity, whereas the small triangular islands appear as not so deep dips, suggesting an optical resolution better than the triangular island size. In order to estimate the resolution in the optical image, we calculated the Fourier spectrum along the fast scan direction for each scan line and then summed the spectra together. The frequency at which the Fourier spectrum drops below the noise level was taken as the resolution of the image.[32,33] Based on this Fourier spectrum criteria, we estimate the resolution to be on the order of 80 nm.

VI. DISCUSSION

In summary, we have presented a novel SNOM/confocal optical microscope design based on design principles of high resolution AFMs. It uses normal force distance regulation and etched fiber tips which are bent into a cantilever geometry. SEM images were presented of tips etched in various etchants, the best results being obtained with pure 50% HF. The roughness on the tip cone surfaces was shown to be due to the etch process in the meniscus, not by the etching *per se*. Simultaneously acquired topographical and near-field optical images of a latex sphere shadow mask sample were presented. The topographical images were acquired in constant gap width mode, the near-field optical images in constant height mode, allowing for a subsequent separation of topographically induced and pure absorption contrast. The near-field optical images show a resolution on the order of 80 nm.

ACKNOWLEDGMENTS

The authors are grateful to E. Poblenz for etching the tips, A. Laws for evaporation of the Al-films, Dr. S. Rogaschewski (Humboldt University Berlin) for the SEM images and Dr. J. Labs and Dr. D. Krabe (IZM Berlin, Fraunhofer Gesellschaft) for the bending of the fibers. The project has been supported in part by SFB 448 and the TMR Network SISITOMAS.

[1] B. Hecht, H. Bielefeldt, Y. Inouye, D. W. Pohl, and L. Novotny, J. Appl. Phys. **81**, 2492 (1997).
[2] L. Novotny, B. Hecht, and D. W. Pohl, Ultramicroscopy **71**, 341 (1998).
[3] E. Betzig, P. L. Finn, and J. S. Weiner, Appl. Phys. Lett. **60**, 2484 (1992).
[4] R. Toledocrow, P. C. Yang, Y. Chen, and M. Vaeziravani, Appl. Phys. Lett. **60**, 2957 (1992).
[5] K. Karrai and R. D. Grober, Ultramicroscopy **61**, 197 (1995).
[6] H. Muramatsu, N. Chiba, T. Ataka, H. Monobe, and M. Fujihira, Ultramicroscopy **57**, 141 (1995).
[7] H. Muramatsu, N. Chiba, and M. Fujihira, Appl. Phys. Lett. **71**, 2061 (1997).
[8] A. Lewis, K. Lieberman, N. Benami, G. Fish, E. Khachatryan, U. Benami, and S. Shalom, Ultramicroscopy **61**, 215 (1995).
[9] C. E. Talley, G. A. Cooksey, and R. C. Dunn, Appl. Phys. Lett. **69**, 3809 (1996).
[10] R. Brunner, A. Bietsch, O. Hollricher, and O. Marti, Rev. Sci. Instrum. **68**, 1769 (1997).
[11] P. K. Hansma, J. P. Cleveland, M. Radmacher, D. A. Walters, P. E. Hillner, M. Bezanilla, M. Fritz, D. Vie, and H. G. Hansma, Appl. Phys. Lett. **64**, 1738 (1994).
[12] E. Oesterschulze, O. Rudow, C. Mihalcea, W. Scholz, and S. Werner, Ultramicroscopy **71**, 85 (1998).
[13] M. Abraham, W. Ehrfeld, M. Lacher, K. Mayr, W. Noell, P. Guthner, and J. Barenz, Ultramicroscopy **71**, 93 (1998).
[14] K. H. Besocke, Surf. Sci. **181**, 145 (1987).
[15] J. Frohn, J. F. Wolf, K. H. Besocke, and M. Teske, Rev. Sci. Instrum. **60**, 1200 (1989).
[16] J. F. Wolf, Ph.D. thesis, RWTH Aachen, published as Jül-Bericht 2391 Forschungszentrum Jülich, 1990.
[17] S. Horch, P. Zeppenfeld, R. David, and G. Comsa, Rev. Sci. Instrum. **65**, 3204 (1994).
[18] M. Bott, T. Michely, and G. Comsa, Rev. Sci. Instrum. **66**, 4135 (1995).
[19] G. Meyer, Rev. Sci. Instrum. **67**, 2960 (1996).
[20] S. Behler, M. K. Rose, J. C. Dunphy, D. F. Ogletree, M. Salmeron, and C. Chapelier, Rev. Sci. Instrum. **68**, 2479 (1997).
[21] J. P. Cleveland, T. E. Schaffer, and P. K. Hansma, Phys. Rev. B **52**, R8692 (1995).
[22] B. Hecht, H. Bielefeldt, L. Novotny, Y. Inouye, and D. W. Pohl, Phys. Rev. Lett. **77**, 1889 (1996).
[23] C. Lienau, A. Richter, and T. Elsaesser, Appl. Phys. Lett. **69**, 325 (1996).
[24] E. Betzig, J. K. Trautman, T. D. Harris, J. S. Weiner, and R. L. Kostelak, Science **251**, 1468 (1991).
[25] D. Zeisel, S. Nettesheim, B. Dutoit, and R. Zenobi, Appl. Phys. Lett. **68**, 2491 (1996).
[26] D. R. Turner, U.S. Patent 4,469,554 (1983).

[27] A. Sayah, C. Philipona, P. Lambelet, M. Pfeffer, and F. Marquisweible, Ultramicroscopy **71**, 59 (1998).
[28] H. M. Marchman, J. E. Griffith, and R. W. Filas, Rev. Sci. Instrum. **65**, 2538 (1994).
[29] T. Lacoste, T. Huser, R. Prioli, and H. Heinzelmann, Ultramicroscopy **71**, 333 (1998).
[30] K. Nakajima, Y. Mitsuoka, N. Chiba, H. Muramatsu, T. Ataka, K. Sato, and M. Fujihira, Ultramicroscopy **71**, 257 (1998).
[31] U. Ch. Fischer and H. P. Zingsheim, J. Vac. Sci. Technol. **19**, 881 (1981).
[32] H.-J. Butt, R. Guckenberger, and J. P. Rabe, Ultramicroscopy **46**, 375 (1992).
[33] D. Barchiesi, Microsc. Microanal. Microstruct. **8**, 1 (1997).